Preprint Title	Design and synthesis of axially chiral platinum(II) complex and its CPL properties in PMMA matrix
Authors	Daiki Tauchi, Sota Ogura, Misa Sakura, Kazunori Tsubaki and Masashi Hasegawa
Publication Date	01 Sept. 2025
Article Type	Full Research Paper
Supporting Information File 1	Supporting Information.docx; 4.1 MB
ORCID® iDs	Daiki Tauchi - https://orcid.org/0009-0007-5434-2590

Design and synthesis of axially chiral platinum(II) complex and its CPL properties in PMMA matrix

Daiki Tauchi*[1], Sota Ogura[1], Misa Sakura[2], Kazunori Tsubaki[2] and Masashi Hasegawa*[1]

Address: [1]Department of chemistry, Kitasato University, *Kanagawa 252-0373, Japan* and [2] *Graduate School of Life and Environmental Science*, *Kyoto Prefectural University*, *Kyoto 606-8522, Japan*

Email: Daiki Tauchi – tauchi.daiki@kitasato-u.ac.jp

* Corresponding author

Abstract

A pair of axially chiral platinum(II) complex was synthesized via Sonogashira coupling and subsequent coordination of a pincer ligand to a precursor. The complex exhibited a broad absorption band ranging from 250 to 700 nm in the UV–vis spectrum, with TD-DFT calculations indicating mixed ligand-to-ligand charge transfer (LL′CT) and metal-to-ligand charge transfer (MLCT) character. Photoluminescence measurements in CH_2Cl_2 solution revealed dual emission peaks at 427 nm and 596 nm, with a quantum yield of 3%. In PMMA matrix, the emission peaks were blue-shifted to 408 nm and 558 nm, and the quantum yield slightly increased to 4%. CD spectra showed distinct Cotton effects in the MLCT region, and CPL signals were observed only in the PMMA matrices, with a dissymmetry factor (g_{lum}) of $|0.4 \times 10^{-3}|$. These results demonstrate that axial

chirality can be effectively transferred to the metal center and induce CPL activity under restricted molecular motion, providing a promising strategy for designing chiral phosphorescent materials.

Keywords

axial chirality; circularly polarized luminescence (CPL); platinum(II) complex; phosphorescence; chiral chemistry

Introduction

Luminescent materials based on metal complexes have been extensively studied due to their high phosphorescence efficiency, making them promising candidates for applications in organic light-emitting diodes (OLEDs) [1-5], sensors [6-9], and bioimaging materials [10,11]. Among these materials, pincer-type platinum(II) complexes have attracted particular attention, owing to the structural robustness imparted by tridentate chelating ligands and their excellent luminescent properties[12-17]. These complexes have been widely investigated, not only for practical application but also from the perspective of fundamental chemistry.

In recent years, the design and synthesis of luminescent pincer-type platinum(II) metal complexes incorporating chirality, as well as the study of their physicochemical properties, have gained significant interest [18-23]. Such efforts aim to explore the development of materials exhibiting circulaly polarized luminescence (CPL). However, most reported chiral pincer-type platinum(II) complexes utilize point chirality as the chiral element. For instance, Zhong and co-workers reported a chiral platinum(II) complex bearing a leucine-derived pendant group, which exhibited aggregation-enhanced red phosphorescence and CPL properties in the solid states [20], while Yam

and co-workers also reported pincer-type platinum(II) complexes containing chiral amine moieties, and investigated their aggregation behavior and chiroptical properties [22]. In both cases, significant CPL signals were observed only in the aggregated state, because the introduction of chirality through point chirality does not induce a significant electronic effect in the monomeric state; instead, the observed chiroptical activity originates from the chiral spatial arrangement of several molecules in the aggregated state. To expand the scope of chirality in metal complex chemistry with pincer ligand and to facilitate the design of next-generation CPL-active materials, alternative chiral motifs beyond point chirality are highly desirable.

Herein, we report the designed and synthesis of a chiral ligand featuring an axially chiral binaphthyl backbone and employed it in the construction of novel types of chiral platinum(II) complex with pincer ligand (Figure 1). We investigated the spectroscopic properties of the resulting complex, including its chiroptical behavior, through a combination of experimental measurements and density functional theory (DFT) calculations. The experimental UV–vis spectrum was in good agreement with the DFT calculations, revealing that the electronic transitions originate from both ligand-to-ligand charge transfer (LL'CT) and MLCT. Furthermore, chiroptical measurements by circular dichroism (CD) and CPL spectroscopy indicated that the axial chirality of the binaphthyl moiety is effectively transferred to the pincer unit in both the ground and excited states, particularly within the metal-to-ligand charge transfer (MLCT) band. While no CPL was observed in solution, distinct CPL properties observed in the PMMA matrices. This behavior is attributed to the effect of the axial chirality, which becomes more effective upon suppression of molecular motion within the polymer environment.

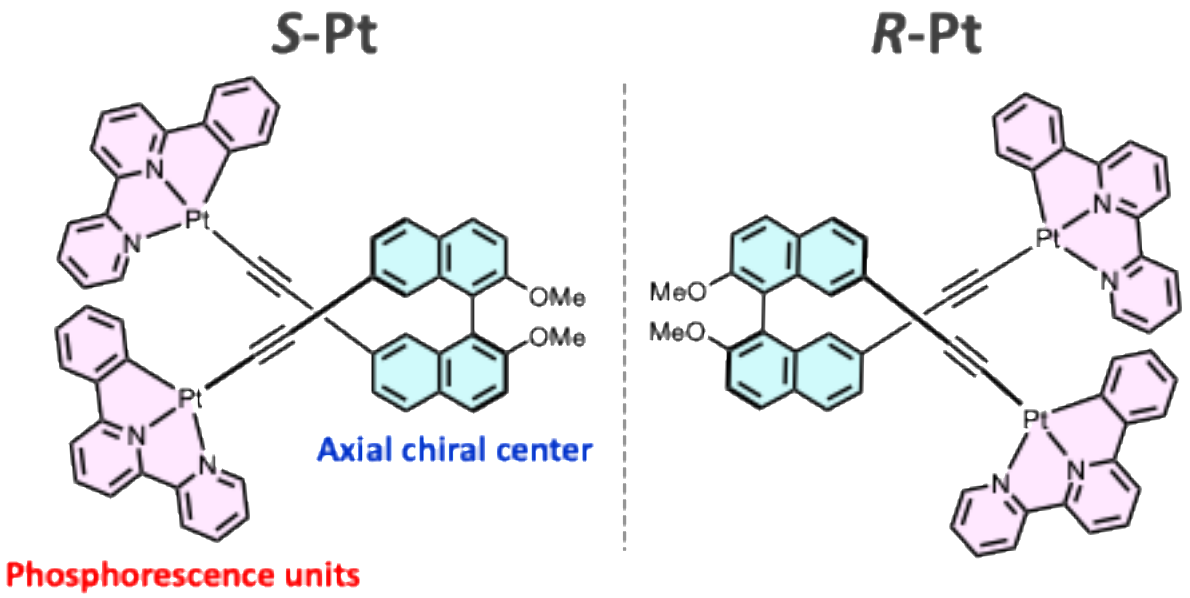

Figure 1 Molecular design for axially chiral platinum(II) complex (***S/R*-Pt**) based on pincer ligand.

Synthesis

Scheme1 Synthesis of binaphthyl based ligand and platinum(II) complex. Yields indicated correspond to the *S*-isomer.

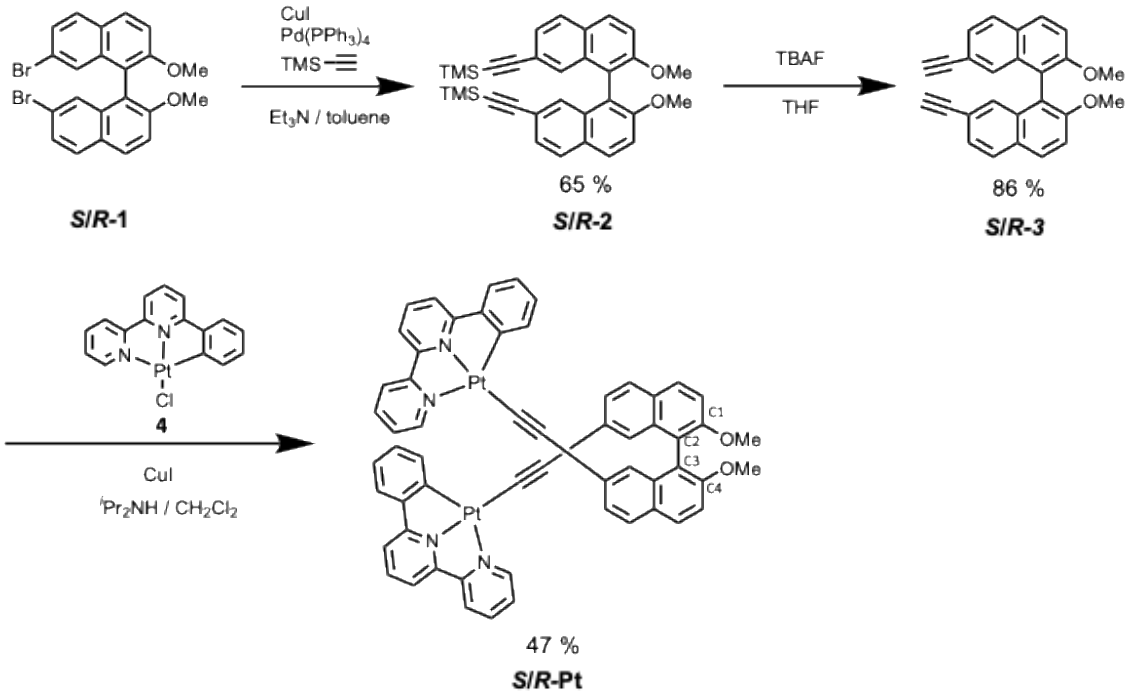

Each enantiomer of the target platinum(II) complex was synthesized separately. The synthesis of the chiral backbone ***S*/*R*-3** was prepared in two steps starting from a chiral binaphthyl derivative [24]. Compound ***S*/*R*-2** was obtained by using a Sonogashira coupling reaction of ***S*/*R*-1** with trimethtylsilylacetylene in toluene. Subsequent deprotection of the trimethylsilyl (TMS) groups with tetrabutylammonium fluoride (TBAF) afforded the desired ligand of ***S*/*R*-3**. The preparation of the target Pt(II) complex was prepared by using a similar procedure of the other Pt complex with pincer ligand moieties[25]. Thus, the reaction of ***S*/*R*-3** with platinum(II) precursor (**4**) in the presence of CuI and diisopropylamine afforded the target platinum(II) complex ***S*/*R*-Pt** in moderated yield. The identification of the complex ***S*/*R*-Pt** were carried out with ^{1}H and ^{13}C NMR spectroscopy, as well as high-resolution mass spectrometry (HRMS). Due to its low solubility, single crystals suitable for X-ray crystallographic analysis could not be obtained.

Spectroscopic analysis and DFT calculations

To elucidate the electronic structure of the platinum(II) complex, UV–vis absorption spectroscopy was performed in dilute solution of dichloromethane (1.0×10^{-5} M) (Figure2 (a)). The absorption spectrum displayed wide range absorption character from 250 to 700 nm with maxima at 430, 331, and 276 nm. To gain deeper insight into the nature of these electronic transitions, density functional theory (DFT) calculations were carried out. The calculations were performed at the CAM-B3LYP/6-31G+(d,p) level, with the LANL2DZ basis set applied to the Pt atoms. The optimized structure of ***R*-Pt** is shown in Figure 2 (b). The dihedral angle of the binaphthyl moiety (∠C1-C2-C3-C4) was 71°, which is smaller than the 80–100° range typically reported for the most stable conformation of binaphthyl groups [26]. In contrast, the dihedral angles

between the binaphthyl unit and the coordination plane were 54° and 52°, respectively. The UV-Vis spectral simulation based on electronic transition obtained from time-dependent (TD)-DFT qualitatively reproduced the observed spectra. The detail of the electronic transition was attached Supporting Information. The broad absorption band in the long-wavelength region was assigned to a MLCT transition, while the absorption bands in the shorter wavelength region were attributed to a mixture LL'CT and MLCT transitions. These electronic characteristics are similar to those reported for other chiral platinum(II) complexes [27-29].

(a)

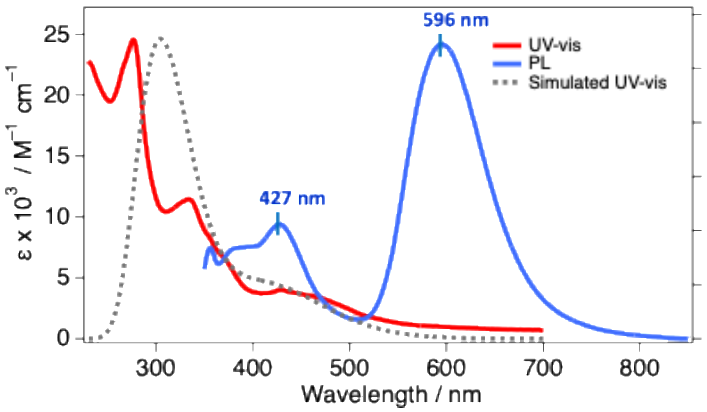

(b)

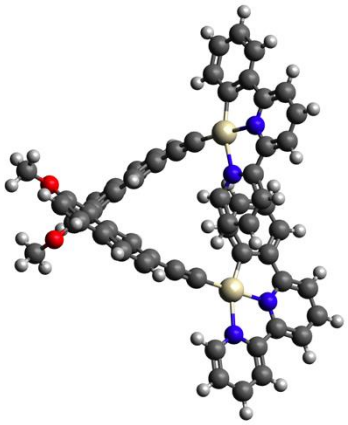

Figure 2 (a) UV-vis and PL spectra (λ_{ex} = 300 nm) in 1.0 × 10^{-5} M dichloromethane solution, gray dotted line shows simulated UV-vis spectrum by TD-DFT calculation. (b) Optimized structure of ***R*-Pt** by DFT calculation.

The photoluminescence (PL) spectrum of the platinum(II) complex was measured in dichloromethane solution (1.0 × 10^{-5} M), revealing two emission bands centered at approximately 427 nm and 596 nm (Figure 2). The corresponding emission decays were well fitted by a three-exponential function, yielding fluorescence components of 3.6 ns (62%), 8.0 ns (20%), and 0.39 ns (18%) at 427 nm, and phosphorescence

components of 0.11 μs (64%), 69 ns (35%), and 6.3 ns (1%) at 596 nm, respectively. The photoluminescence quantum yield (PLQY) in dichloromethane was measured to be 3%. The relatively low PLQY is likely attributed to non-radiative deactivation pathways associated with rotational motions of the axially chiral moiety and the ethynyl-linked coordination sites. Therefore, we prepared polymer matrix of PMMA containing 1wt% of ***S*/*R*-Pt** to investigate the emission behavior under conditions where molecular motion was suppressed.

The PMMA matrix was obtained by dissolving ***S*/*R*-Pt** and PMMA in chloroform under heating at 40 °C, casting the solution onto a glass substrate, and allowing it to dry slowly under ambient conditions. The emission spectrum of the PMMA matrix exhibited two emission components, similar to those observed in solution (Figure 3). Compared to the solution phase, the longer-wavelength emission peak (558 nm) was blue-shifted by 38 nm, and the shorter-wavelength emission peak (408 nm) was blue-shifted by 19 nm. These hypsochromic shifts are attributed to due to the more hydrophobic environment surrounding the complex in PMMA matrix. The PLQY in the PMMA matrix was 4%, comparable to that observed in solution. In the film, the emission lifetimes could be fitted with double- or triple-exponential functions, resulting in fluorescence components of 0.49 ns (50%) and 0.48 ns (50%) at 408 nm, and phosphorescence components of 0.25 μs (76%), 0.024 μs (11%), and 2.8 ns (10%) at 558 nm, consistent with similar excited-state dynamics in both environments.

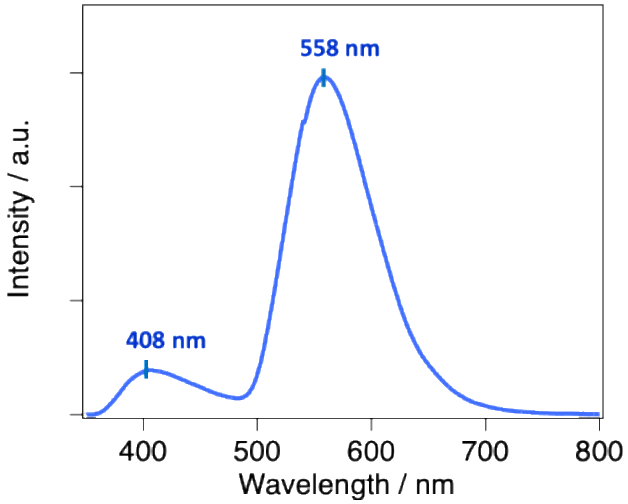

Figure 3 Emission spectrum of 1wt% PMMA matrix (***R*-Pt**) (λ_{ex} = 300 nm)

To investigate the chiroptical properties of the complex, CD spectra were recorded in 1.0 × 10^{-5} M dichloromethane solution (Figure 4 (a)). The CD spectra of the both enantiomers showed clear mirror-image signals, and the experimental results were in good agreement with the simulated spectra obtained from DFT calculations (see SI). The first Cotton effect attributed by MLCT transition was observed around 400 to 500 nm, indicating the axial chirality of binaphthyl groups reflect the CD signals. It assumes circularly polarized phosphorescence (CPP) properties by platinum(II) centered emission. The TD-DFT calculation also reproduces the CD spectrum, showing the same sign in the first Cotton effect (see SI). The CPL measurements were conducted to further elucidate the chiral emissive properties of the platinum(II) complex. While the dichloromethane solution of the complex showed no detectable CPL signal, this is likely due to averaging of the transition dipole moments caused by intramolecular motions, leading to a cancellation of dipole moment or potentially weak magnetic dipole moment. In contrast, 1wt% PMMA matrices exhibited distinct CPL activity, with the CPL signal showing the same sign as the first Cotton effect in the CD spectrum (Figure 4 (b)). The measured dissymmetry factor $|g_{lum}|$ was 0.4 × 10^{-3}, which is within the

typical range for organic small-molecule systems, indicating the restriction of molecular motions in PMMA matrices induced CPL properties.

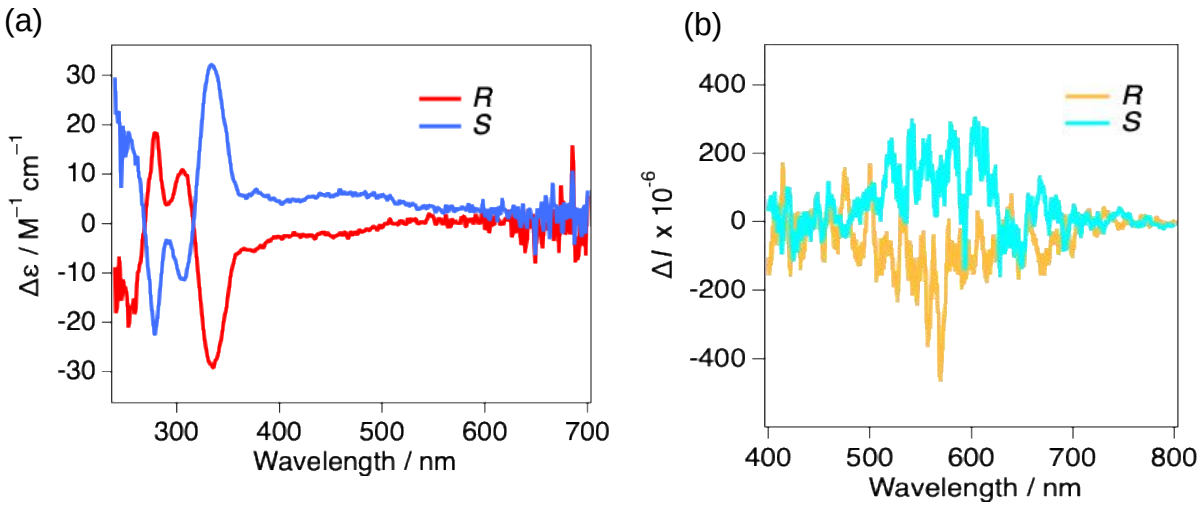

Figure 4 (a) CD spectra of ***S/R*-Pt** in 1.0 × 10^{-5} M dichloromethane solution. (b) CPL spectra of 1wt% PMMA film (λ_{ex} = 300 nm)

Conclusion

In conclusion, we synthesized a novel pincer-type platinum(II) complex by incorporating an axially chiral binaphthyl ligand through an acetylene linker. Spectroscopic and theoretical analyses revealed that the axial chirality of the binaphthyl moiety effectively induces chirality in the platinum center, particularly within the MLCT band. The complex exhibited dual emission and distinct CPL activity in PMMA matrices, with a dissymmetry factor of $|0.4 \times 10^{-3}|$, highlighting the role of restricted molecular motion in enhancing chiroptical properties. These findings underscore the potential of axial chirality as a design principle for developing chiral phosphorescent materials and open avenues for further exploration of chiral metal complexes in optoelectronic applications.

Experimental

・General information

All reagents and solvents were of the commercial reagent grade and used without further purification. Dichloromethane for spectroscopy was purchased from FUJIFILM Wako Pure Chemical Corporation. All the compounds were identified by ^{1}H- , ^{13}C-NMR and ESI-MS. ^{1}H- and ^{13}C-NMR spectra were recorded on a BRUKER AVANCE III 400 at 25 °C in *d*-chloroform or d_6-DMSO. ^{1}H-NMR chemical shifts are expressed in parts per million (δ) relative to trimethyl silane (TMS) as a reference. Mass spectra were obtained with a Thermo Scientific, Exactive Plus Orbitrap Mass Spectrometer for electrospray ionization (ESI). IR spectra were measured using a FT/IR-4600 with KBr pellet. UV-vis absorption spectra of CH_2Cl_2 solutions (1.0×10^{-5} M) were recorded with JASCO V-560 UV-vis spectrometer. Photoluminescence spectra of CH_2Cl_2 solutions

(1.0 × 10^{-5} M) and the 1wt% PMMA matrices were acquired using JASCO FP-8550 spectrometer at room temperature, at excitation wavelength of 300 nm (both solutions and PMMA matrix). CPL spectra of CH_2Cl_2 solutions (1.0 × 10^{-5} M) and the 1wt% PMMA matrices were measured with a JASCO CPL-300 spectrofluoropolarimeter at room temperature, at a scattering angle of 0° upon excitation with unpolarized, monochromated incident light. Absolute PLQYs of solutions and powder samples were determined using a JASCO FP-8550 spectrometer with an integrating sphere (JASCO ILF-533, diameter 96 mm) at excitation wavelength of 300 nm. Fluorescence lifetimes were measured for solutions and powder samples with a HORIBA DeltaFlex spectrometer with a 370 nm LED light source for excitation. For the lifetime measurements of solution, a conventional 1 cm quartz cell was used. All calculations were performed by using Gaussian 16 rev C.02 program package. The density functional theory (DFT) at the level of CAM-B3LYP/LANL2DZ for Pt atoms. The Optimized equilibrium structures were confirmed by normal coordinate analyses, with no imaginary frequency found.

・Synthesis of axially chiral ligand and Pt(II) complex

・Synthesis of ***S*/*R*-2**

The following describes the procedure for the *S*-enantiomer. Under an argon atmosphere, a mixture of ***S*-1** (282 mg, 0.597 mmol), CuI (32 mg, 0.17 mmol), $Pd(PPh_3)_4$ (112 mg, 0.0962 mmol) and trimethylsilylacetylene (0.40 mL, 2.9 mmol) was added degassed solution of Et_3N (2.6 mL, 19 mmol) and toluene (5.2 mL) by argon bubbling. The reaction mixture was refluxed at 90 °C for 21 hours. After cooling to room temperature, the reaction mixture was filtered through Celite. The Celite was

thoroughly washed with dichloromethane, and the combined filtrate was washed three times with saturated aqueous NH_4Cl and brine. The organic layer was dried over anhydrous sodium sulfate. The crude product was purified by silica gel column chromatography using a 1:1 mixture of dichloromethane and hexane as the eluent. The eluent was evaporated to give the off-white solid ***S*-2** (197 mg, 65%).

Data for ***S*-2**: Off white solid; M.p. 103℃ (decomp.); HRMS (orbitrap) *m/z* calcd. for $C_{32}H_{34}O_2Si_2$ $[M + H]^+$: 529.1990, Found 529.1990; ^{1}H NMR (400 MHz, $CDCl_3$) δ 7.94 (d, *J* = 9.2 Hz, 2H), 7.79 (d, *J* = 8.4 Hz, 2H), 7.45 (d, *J* = 8.8 Hz, 2H), 7.36 (dd, *J* = 1.6, 8.4 Hz, 2H), 7.202-7.198 (m, 2H), 3.74 (s, 6H), 0.17 (s, 18H); ^{13}C NMR (150 MHz, $CDCl_3$) δ 155.5, 133.7, 129.4, 128.9, 128.7, 128, 126.7, 121, 119.1, 114.7, 106.1, 94.2, 56.6, 0.05; IR (KBr) ν_{MAX} = 3058, 1774, 1409, 1191, 1152, 969, 698, 553, 431 cm^{-1}. The *R*-isomer was synthesized using a similar procedure to that of the *S*-isomer, except that compound ***R*-1** (300 mg, 0.52 mmol), trimethylsilylacetylene (0.30 mL, 2.2 mmol), CuI (32 mg, 0.17 mmol), $Pd(PPh_3)_4$ (112 mg, 0.096 mmol), Et_3N (2.3 mL) in toluene (4.5 mL) were used. The yield was 78%.

・Synthesis of ***S*/*R*-3**

Under an argon atmosphere. ***S*-2** (197 mg, 0.389 mmol) in tetrahydrofuran (1.7 mL) was treated with a dropwise addition of 1M TBAF solution (16.7 mL, 16.7mmol), and the resulting solution was stirred at room temperature for 2 hours. After the addition of water, the mixture was extracted with dichloromethane three times, and the organic layers were washed with saturated brine. The organic layer was dried over anhydrous sodium sulfate, after drying, the solvent was removed under reduced pressure. The crude product was purified by silica gel column chromatography using a 1:1 mixture of dichloromethane and hexane as the eluent. The eluent was evaporated to give the white crystalline solid ***S*-3** (121 mg, 86%).

Data for ***S*-3**: White crystal; M.p. 160℃ (decomp.); HRMS (orbitrap) *m/z* calcd. for $C_{26}H_{18}O_2$ $[M]^+$: 362.1301, Found 362.1299; ^{1}H NMR (400 MHz, $CDCl_3$) δ 7.96 (d, *J* = 8.8 Hz, 2H), 7.81 (d, *J* = 8.4 Hz, 2H), 7.47 (d, *J* = 8.8 Hz, 2H), 7.37 (dd, *J* = 1.6, 8.4 Hz, 2H), 7.26 (s, 2H), 3.76 (s, 6H), 2.95 (s, 2H); ^{13}C NMR (150 MHz, $CDCl_3$) δ 155.5, 133.5, 129.5, 129.4, 128.8, 128.2, 126.4, 119.9, 118.9, 114.9, 84.6, 77.1 56.7; IR(KBr) ν_{MAX} = 3238, 2938, 2839, 2457, 1352, 1320, 1171, 1152, 961, 882, 597, 530, 432 cm^{-1}.

The *R*-isomer was synthesized using a similar procedure to that of the *S*-isomer, except that compound ***R*-2** (208 mg, 0.41 mmol) and TBAF (1.7 mL) in THF (17 mL) were used. The yield was 81%.

・Synthesis of ***S*/*R*-Pt**

The synthesis of platinum(II) complex describe *R*-enantiomer. Under an argon atmosphere, a mixture of ***R*-3** (16 mg, 0.043 mmol), **4** (39 mg, 0.084 mmol), and CuI (2.4 mg, 0.013 mmol) were dissolved in degassed solvent of dichloromethane (10 mL) and diisopropylamine (10 mL). The reaction mixture was refluxed at 90 °C for 28 hours. After cooling to room temperature, water was added, and the mixture was extracted three times with dichloromethane and saturated aqueous NH_4Cl. The organic layers were washed with saturated brine, then dried over anhydrous sodium sulfate. After drying the solvent was removed under reduced pressure. Crude product was then purified by silica gel column chromatography using a 9:1 mixture of dichloromethane and methanol as the eluent. The eluate was evaporeted, and the resulting solid was washed with methanol and dried under vacuum to afford the orange solid ***R*-Pt** (24 mg, 47%).

Data for ***R*-Pt**: Orange solid; M.p. 280°C (decomp.); HRMS (orbitrap) *m/z* calcd. for $C_{58}H_{38}N_4O_2Pt_2$ $[M+H]^+$: 1212.2343, Found 1212.2342; ^{1}H NMR (400 MHz, DMSO-d_6) δ 8.81 (d, *J* = 5.2 Hz, 2H), 8.41 (d, *J* = 8.0 Hz, 2H), 8.25 (t, *J* = 8.0 Hz, 2H), 8.14 (d, *J* = 8.0 Hz, 2H), 8.00-8.07 (m, 4H), 7.93 (d, *J* = 8.0 Hz, 2H), 7.85 (d, *J* = 8.4 Hz, 2H), 7.67-7.75 (m, 2H), 7.50-7.57 (m, 6H), 7.32 (dd, *J* = 1.2 and 8.4 Hz, 2H), 7.20-6.95 (m, 6H), 3.77 (s, 6H); ^{13}C NMR (100 MHz, DMSO-d_6) δ 164.1, 157.6, 155.0, 154.0, 150.8, 147.1, 142.2, 140.1, 137.6, 133.7, 130.7, 129.1, 128.5, 127.8, 127.2, 126.8, 126.7, 126.1, 125.0, 124.1, 123.6, 119.3, 119.2, 117.9, 113.4, 110.1, 109.5, 106.2, 56.3; IR(KBr) ν_{MAX} = 3448, 3061, 2923, 2846, 2371, 2345, 2091, 1610, 1499, 1458, 1255, 1092, 880, 835, 757, 477 cm^{-1}.

The ***S*-Pt** complex was synthesized using a similar procedure to that of the ***S*-Pt** complex, except that compound ***R*-3** (20 mg, 0.056 mmol), **4** (51 mg, 0.11 mmol), ^{i}PrNH (4 mL) in CH_2Cl_2 (16 mL) were used. The yield was 20%.

Supporting Information

Supporting information text was attached.

Acknowledgements

The authors are grateful to Prof. Dr. Takahiro Tsuchiya and Dr. Masfumi Ueda (Kitasato University) for their helpful discussion. We would also like to thank Ms. Chika Hasegawa for her assistance in the synthesis of part of the axially chiral binaphthyl units.

Funding

This work was supported by Grant-in-Aid for Research Activity Start-up (T.D., Grant number 25K23609) and CREST from Japan Science and Technology Agency (M.H., (Grant Number JP-MJCR2001). This work was also partly supported by Kitasato University Research Grant for Young Researchers.

References

1. Rashamuse, T. J.; Mohlala, R. L.; Coyanis, E. M.; Magwa, N. P. *Molecules* **2023**, *28*, 5272. doi:10.3390/molecules28135272
2. Li, X.; Xie, Y.; Li, Z. *Chemistry An Asian Journal* **2021**, *16*, 2817–2829. doi:10.1002/asia.202100784
3. Li, S.; Zhou, L.; Zhang, H. *Light Sci Appl* **2022**, *11*. doi:10.1038/s41377-022-00866-w
4. Kourkoulos, D.; Karakus, C.; Hertel, D.; Alle, R.; Schmeding, S.; Hummel, J.; Risch, N.; Holder, E.; Meerholz, K. *Dalton Trans.* **2013**, *42*, 13612. doi:10.1039/c3dt50364j
5. Li, G.; Zhao, X.; Fleetham, T.; Chen, Q.; Zhan, F.; Zheng, J.; Yang, Y.-F.; Lou, W.; Yang, Y.; Fang, K.; Shao, Z.; Zhang, Q.; She, Y. *Chem. Mater.* **2020**, *32*, 537–548. doi:10.1021/acs.chemmater.9b04263
6. Demas, J. N.; DeGraff, B. A. *J. Chem. Educ.* **1997**, *74*, 690. doi:10.1021/ed074p690
7. Higgins, B.; DeGraff, B. A.; Demas, J. N. *Inorg. Chem.* **2005**, *44*, 6662–6669. doi:10.1021/ic050044e
8. Dey, N.; Biswakarma, D.; Bhattacharya, S. *ACS Sustainable Chem. Eng.* **2019**, *7*, 569–577. doi:10.1021/acssuschemeng.8b04107
9. Singh, J.; Yadav, M.; Singh, A.; Singh, N. *Dalton Trans.* **2015**, *44*, 12589–12597. doi:10.1039/c5dt01063b
10. Zhao, Q.; Huang, C.; Li, F. *Chem. Soc. Rev.* **2011**, *40*, 2508. doi:10.1039/c0cs00114g
11. Lee, L. C.-C.; Lo, K. K.-W. *Chem. Rev.* **2024**, *124*, 8825–9014. doi:10.1021/acs.chemrev.3c00629
12. Wong, K. M.-C.; Tang, W.-S.; Lu, X.-X.; Zhu, N.; Yam, V. W.-W. *Inorg. Chem.* **2005**, *44*, 1492–1498. doi:10.1021/ic049079p
13. Lu, W.; Mi, B.-X.; Chan, M. C. W.; Hui, Z.; Che, C.-M.; Zhu, N.; Lee, S.-T. *J. Am. Chem. Soc.* **2004**, *126*, 4958–4971. doi:10.1021/ja0317776
14. Chow, P.; Cheng, G.; Tong, G. S. M.; To, W.; Kwong, W.; Low, K.; Kwok, C.; Ma, C.; Che, C. *Angew Chem Int Ed* **2015**, *54*, 2084–2089. doi:10.1002/anie.201408940
15. Li, K.; Zou, T.; Chen, Y.; Guan, X.; Che, C. *Chemistry A European J* **2015**, *21*, 7441–7453. doi:10.1002/chem.201406453
16. Albrecht, M.; Van Koten, G. *Angew. Chem. Int. Ed.* **2001**, *40*, 3750–3781. doi:10.1002/1521-3773(20011015)40:20<3750::aid-anie3750>3.0.co;2-6

17. Dikova, Y. M.; Yufit, D. S.; Williams, J. A. G. *Inorg. Chem.* **2023**, *62*, 1306–1322. doi:10.1021/acs.inorgchem.2c04116
18. Gong, Z.-L.; Zhong, Y.-W. *Sci. China Chem.* **2021**, *64*, 788–799. doi:10.1007/s11426-020-9911-4
19. Ikeda, T.; Takayama, M.; Kumar, J.; Kawai, T.; Haino, T. *Dalton Trans.* **2015**, *44*, 13156–13162. doi:10.1039/c5dt01284h
20. Gong, Z.; Dan, T.; Yao, J.; Zhong, Y. *ChemPhotoChem* **2022**, *6*. doi:10.1002/cptc.202100239
21. Zhang, X.-P.; Chang, V. Y.; Liu, J.; Yang, X.-L.; Huang, W.; Li, Y.; Li, C.-H.; Muller, G.; You, X.-Z. *Inorg. Chem.* **2015**, *54*, 143–152. doi:10.1021/ic5019136
22. Li, B.; Li, Y.; Chan, M. H.-Y.; Yam, V. W.-W. *J. Am. Chem. Soc.* **2021**, *143*, 21676–21684. doi:10.1021/jacs.1c10943
23. Tian, Y.; Chen, B.; Jiang, S.; Yuan, M.; Ren, J.; Wang, F. *Chem. Commun.* **2021**, *57*, 11996–11999. doi:10.1039/d1cc04806f
24. Nojima, Y.; Hasegawa, M.; Hara, N.; Imai, Y.; Mazaki, Y. *Chem. Commun.* **2019**, *55*, 2749–2752. doi:10.1039/c8cc08929a
25. Dikova, Y. M.; Yufit, D. S.; Williams, J. A. G. *Inorg. Chem.* **2023**, *62*, 1306–1322. doi:10.1021/acs.inorgchem.2c04116
26. Nishizaka, M.; Mori, T.; Inoue, Y. *J. Phys. Chem. A* **2011**, *115*, 5488–5495. doi:10.1021/jp202776g
27. Biet, T.; Cauchy, T.; Sun, Q.; Ding, J.; Hauser, A.; Oulevey, P.; Bürgi, T.; Jacquemin, D.; Vanthuyne, N.; Crassous, J.; Avarvari, N. *Chem. Commun.* **2017**, *53*, 9210–9213. doi:10.1039/C7CC05198K
28. Inoue, R.; Kondo, R.; Morisaki, Y. *Chem. Commun.* **2020**, *56*, 15438–15441. doi:10.1039/D0CC06205G
29. Ikeshita, M.; Shimizu, I.; Watanabe, S.; Yamada, T.; Suzuki, S.; Tanaka, S.; Hattori, S.; Shinozaki, K.; Imai, Y.; Tsuno, T. *Inorg. Chem.* **2024**, *63*, 23642–23650. doi:10.1021/acs.inorgchem.4c03675